(12) INTERNATIONAL APPLICATION PUBLISHED UNDER THE PATENT COOPERATION TREATY (PCT)

(19) World Intellectual Property Organization
International Bureau

(43) International Publication Date
27 December 2007 (27.12.2007)

PCT

(10) International Publication Number
WO 2007/149055 A1

(51) International Patent Classification:
G02B 6/125 (2006.01) *G02B 6/122* (2006.01)

(21) International Application Number: PCT/SG2007/000174

(22) International Filing Date: 21 June 2007 (21.06.2007)

(25) Filing Language: English

(26) Publication Language: English

(30) Priority Data:
60/815,317 21 June 2006 (21.06.2006) US

(71) Applicant *(for all designated States except US)*: **AGENCY FOR SCIENCE, TECHNOLOGY AND RESEARCH** [SG/SG]; 20 Biopolis Way, #07-01 Centros, Singapore 138668 (SG).

(72) Inventors; and
(75) Inventors/Applicants *(for US only)*: **PNG, Jason** [SG/SG]; c/o Institute of High Performance Computing1 Scieence Park Road, #01-01, The Capricon, Singapore Science Park II, Singapore 117528 (SG). **LIM, Soon Thor** [SG/SG]; c/o Institute of High Performance Computing1 Science Park Road, #01-01, The Capricorn, Singapore Science Park II, Singapore 117528 (SG).

(74) Agent: **ELLA CHEONG SPRUSON & FERGUSON (SINGAPORE) PTE LTD**; P.O. Box 1531Robinson Road Post Office, Singapore 903031 (SG).

(81) Designated States *(unless otherwise indicated, for every kind of national protection available)*: AE, AG, AL, AM, AT, AU, AZ, BA, BB, BG, BH, BR, BW, BY, BZ, CA, CH, CN, CO, CR, CU, CZ, DE, DK, DM, DO, DZ, EC, EE, EG, ES, FI, GB, GD, GE, GH, GM, GT, HN, HR, HU, ID, IL, IN, IS, JP, KE, KG, KM, KN, KP, KR, KZ, LA, LC, LK, LR, LS, LT, LU, LY, MA, MD, MG, MK, MN, MW, MX, MY, MZ, NA, NG, NI, NO, NZ, OM, PG, PH, PL, PT, RO, RS, RU, SC, SD, SE, SG, SK, SL, SM, SV, SY, TJ, TM, TN, TR, TT, TZ, UA, UG, US, UZ, VC, VN, ZA, ZM, ZW.

(84) Designated States *(unless otherwise indicated, for every kind of regional protection available)*: ARIPO (BW, GH, GM, KE, LS, MW, MZ, NA, SD, SL, SZ, TZ, UG, ZM, ZW), Eurasian (AM, AZ, BY, KG, KZ, MD, RU, TJ, TM), European (AT, BE, BG, CH, CY, CZ, DE, DK, EE, ES, FI, FR, GB, GR, HU, IE, IS, IT, LT, LU, LV, MC, MT, NL, PL, PT, RO, SE, SI, SK, TR), OAPI (BF, BJ, CF, CG, CI, CM, GA, GN, GQ, GW, ML, MR, NE, SN, TD, TG).

Published:
— *with international search report*

[Continued on next page]

(54) Title: PLANAR OPTICAL SPLITTER OR COMBINER AND PASSIVE SENSOR DEVICE

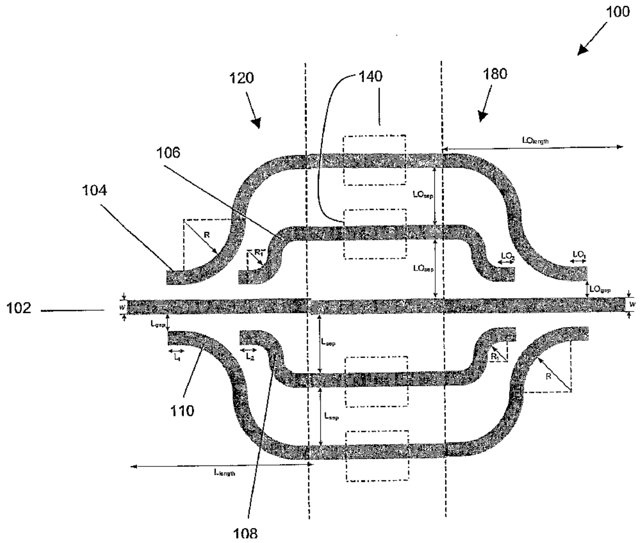

(57) Abstract: An optical splitter, a combiner and a device. The optical splitter comprises a first longitudinal waveguide for receiving an incoming light wave; at least first and second pairs of output waveguides, the output waveguides of each pair being disposed on opposite sides of the first waveguide; wherein each of the output waveguides of each pair comprises a longitudinal portion disposed parallel to the first waveguide and such that optical power is coupled from the first waveguide into the respective longitudinal portions and the longitudinal portions of output waveguides of the first and second pairs are displaced along a length of the first waveguide; wherein each of the output waveguides of each pair further comprises a substantially S-shaped portion continuing from the respective longitudinal portions and such that optical power coupling between the respective S-shaped portions of output waveguides of the first and second pairs is substantially inhibited.

WO 2007/149055 A1

— *before the expiration of the time limit for amending the claims and to be republished in the event of receipt of amendments*

For two-letter codes and other abbreviations, refer to the "Guidance Notes on Codes and Abbreviations" appearing at the beginning of each regular issue of the PCT Gazette.

PLANAR OPTICAL SPLITTER OR COMBINER AND PASSIVE SENSOR DEVICE

FIELD OF INVENTION

The present invention relates broadly to an optical splitter, to an optical combiner, and to an optical device.

BACKGROUND

In recent years, integrated optical devices have received tremendous attention as they provide low cost, high density and high data rate devices for a wide range of applications. Integrated optical devices have also been increasingly used for sensing applications because of their inherent characteristics such as high sensitivity, miniaturisation, mechanical stability and immunity to electromagnetic interference.

Optical device fabrication processes, which adopt planar CMOS technology from the mature microelectronics industry, offer ease of manufacturing and the possibility of simultaneous detection of several analytes on a single chip. Various methods have been implemented for the design of integrated optical biosensors, such as waveguide surface plasmon resonance, waveguide grating coupler, Mach-Zehnder and nanocavity.

For biosensing applications, a number of sensor configurations have been proposed, including Mach-Zehnder interferometer (MZI) and microcavity sensors.

However, most existing proposals are limited to single sensing channels. A multiple sensor device with multiple sensing channels based on such proposals typically requires one light source for each sensing channel.

In realising multiple sensing channel devices using only a single source, existing optical combiner/splitter structures have a number of disadvantages. For example, in one configuration, arrays of interconnected 3-dB couplers may be used to realise nxN couplers. Such a configuration suffers from disadvantages such as high optical losses and an accumulative size of the overall device.

Alternatively, interference based integrated nxN star couplers have been proposed. However, such couplers suffer from high optical losses and complexity of manufacturing.

A need therefore exists to provide an optical combiner/splitter structure that seeks to address at least one of the above disadvantages.

On the other hand, a need also exists to provide an active optical component for use in optical devices such as sensors or communication devices, the active optical component having improved performance in terms of at least one of attenuation and/or driving power.

SUMMARY

In accordance with a first aspect of the present invention there is provided a optical splitter comprising a first longitudinal waveguide for receiving an incoming light wave; at least first and second pairs of output waveguides, the output waveguides of each pair being disposed on opposite sides of the first waveguide; wherein each of the output waveguides of each pair comprises a longitudinal portion disposed parallel to the first waveguide and such that optical power is coupled from the first waveguide into the respective longitudinal portions and the longitudinal portions of output waveguides of the first and second pairs are displaced along a length of the first waveguide; wherein each of the output waveguides of each pair further comprises a substantially S-shaped portion continuing from the respective longitudinal portions and such that optical power coupling between the respective S-shaped portions of output waveguides of the first and second pairs is substantially inhibited.

The longitudinal portions of the output waveguides of each pair may be disposed at substantially a same distance on the opposite sides of the first wav guide.

The longitudinal portions of the output waveguides of both pairs may be disposed at substantially the same distance on the opposite sides of the first waveguide.

A radius of the S-shaped portions of the output waveguides of each pair may be chosen such that optical transmission losses are reduced compared to an angled alignment of waveguide portions.

The optical splitter may be arranged for coupling substantially the same optical power from the light wave into the output waveguides.

Substantially all of an input power of the light wave may be coupled into the output waveguides.

In accordance with a second aspect of the present invention there is provided an optical combiner comprising a first longitudinal waveguide; at least first and second pairs of input waveguides, the input waveguides of each pair being disposed on opposite sides of the first waveguide; wherein each of the input waveguides of each pair comprises a longitudinal portion disposed parallel to the first waveguide and such that optical power is coupled from the respective longitudinal portions into the first waveguide and the longitudinal portions of input waveguides of the first and second pairs are displaced along a length of the first waveguide; wherein each of the input waveguides of each pair further comprises a substantially S-shaped portion continuing from the respective longitudinal portions for receiving respective incoming light waves and such that optical power coupling between the respective S-shaped portions of input waveguides of the first and second pairs is substantially inhibited.

The longitudinal portions of the input waveguides of each pair may be disposed at substantially a same distance on the opposite sides of the first wav guide.

The longitudinal portions of the input waveguides both pairs may be disposed at substantially the same distance on the opposite sides of the first waveguide.

A radius of the S-shaped portions of the input waveguides of each pair may be chosen such that optical transmission losses are reduced compared to an angled alignment of waveguide portions.

Substantially all of respective input powers of the respective light waves may be coupled into the first waveguide.

In accordance with a third aspect of the present invention there is provided a n optical device comprising a waveguide formed on a substrate, the waveguide comprising a photonic bandgap structure including an optical cavity region; a highly doped cathode region formed along the waveguide and adjacent one side of the optical cavity region of the waveguide; a highly doped anode region formed along the waveguide and adjacent an opposite side of the optical cavity region of the waveguide; wherein the cathode region, the optical cavity region and the anode region form a p-i-n diode structure for controlling an attenuation characteristic of the photonic bandgap structure.

In accordance with a fourth aspect of the present invention there is provided a optical device comprising an optical splitter comprising a first longitudinal waveguide for receiving an incoming light wave, at least first and second pairs of output waveguides, the output waveguides of each pair being disposed on opposite sides of the first waveguide, wherein each of the output waveguides of each pair comprises a longitudinal portion disposed parallel to the first waveguide and such that optical power is coupled from the first waveguide into the respective longitudinal portions, and the longitudinal portions of output waveguides of the first and second pairs are displaced along a length of the first waveguide, wherein each of the output waveguides of each pair further comprises a substantially S-shaped portion continuing from the respective longitudinal portions and such that optical power coupling between the respective S-shaped portions of output waveguides of the first and second pairs is substantially inhibited; and a photonic bandgap structure optically connected to each output waveguide of the splitter, each photonic bandgap structure including a microcavity.

The optical device may further comprise an optical combiner comprising a first longitudinal waveguide, at least first and second pairs of input waveguides, the input waveguides of each pair being disposed on opposite sides of the first waveguide, wherein each of the input waveguides of each pair comprises a longitudinal portion disposed parallel to the first waveguide and such that optical power is coupled from the respective longitudinal portions into the first waveguide and the longitudinal portions of input waveguides of the first and second pairs are displaced along a length of the first waveguide, wherein each of the input waveguides of each pair further comprises a substantially S-shaped portion continuing from the respective longitudinal portions for receiving respective incoming light waves and such that optical power coupling between the respective S-shaped portions of input waveguides of the first and second pairs is substantially inhibited; and wherein the photonic bandgap structures are formed in respective optical connections between the output waveguides of the splitter and the input waveguides of the combiner.

In accordance with a fifth aspect of the present invention there is provided a optical device comprising an optical combiner comprising a first longitudinal waveguide, at least first and second pairs of input waveguides, the input waveguides of each pair being disposed on opposite sides of the first waveguide, wherein each of the input waveguides of each pair comprises a longitudinal portion disposed parallel to the first waveguide and such that optical power is coupled from the respective longitudinal portions into the first waveguide and the longitudinal portions of input waveguides of the first and second pairs are displaced along a length of the first waveguide, wherein each of the input waveguides of each pair further comprises a substantially S-shaped portion continuing from the respective longitudinal portions for receiving respective incoming light waves and such that optical power coupling between the respective S-shaped portions of input waveguides of the first and second pairs is substantially inhibited; and a photonic bandgap structure optically connected to each input waveguide of the combiner, each photonic bandgap structure including a microcavity.

BRIEF DESCRIPTION OF THE DRAWINGS

Embodiments of the invention will be better understood and readily apparent to one of ordinary skill in the art from the following written description, by way of example only, and in conjunction with the drawings, in which:

Figure 1 shows a schematic diagram of a passive device built in accordance with one embodiment of the invention.

Figure 2 shows a schematic diagram of an optical splitter.

Figure 3 shows a plot of normalised power against cT.

Figure 4 shows a cross sectional view of a photonic bandgap structure.

Figure 5 shows a plot of transmission and Q factor.

Figure 6 shows a table summarising Q factor and transmission values.

Figure 7 shows a schematic diagram of an optical combiner.

Figure 8 shows a plot of normalised power against cT

Figure 9 shows a schematic diagram of an optical demultiplexer built in accordance with one embodiment of the invention.

Figure 10 shows a schematic diagram of an optical multiplexer built in accordance with one embodiment of the invention.

Figure 11 shows a schematic diagram of an active device built in accordance with one embodiment of the invention.

Figure 12 shows a cross sectional view of a microcavity of an active device.

Figure 13 shows a plot of drive voltage against drive current and a respective change in refractive index, Δn.

Figure 14 shows a plot of attenuation against drive current.

Figure 15 shows a plot of the change in refractive index, Δn, against transient time for an active diode.

Figure 16 shows a schematic diagram of an active phase modulator MZI built in accordance with one embodiment of the invention.

DETAILED DESCRIPTION

Figure 1 shows a schematic diagram of a passive sensor device 100 built in accordance with one embodiment of the invention.

The passive sensor device 100 has an optical splitter 120 at the input end and an optical combiner 180 at the output end.

The passive sensor device 100 shown in Figure 1 is of the 1X4 splitter configuration, where the passive sensor device 100 comprises a central waveguide 102 and four waveguides 104, 106, 108 and 110. A pair of the waveguides 104, 106, 108 and 110 is disposed on each side of the central waveguide 102. A passive photonic bandgap structure 140 is formed in each of the four waveguides 104, 106, 108 and 110 between the optical splitter 120 and the optical combiner 180.

One advantage of using the passive sensor device 100 is that only one light source (broad-band or tunable laser) and one detector is required, whereas conventional devices require individual light sources and detectors for each arm. As such, the passive sensor device 100 arrangement can provide cost savings.

The passive sensor device 100 has a 1x4 splitter configuration. However, it is possible to realise a 1xN splitter configuration with the appropriate design consideration, in different embodiments.

In one embodiment, the passive sensor device 100 has a semiconductor on insulator (SOI) structure, where silicon Si is used for the waveguides 102, 104, 106, 108 and 110. The waveguides 102, 104, 106, 108 and 110 are formed on an insulating SiO_2 layer which is formed on a Si substrate.

The form of the waveguides 102, 104, 106, 108 and 110 depends on the manufacturing material and technology and can consist of any one or more of the following shapes: ridge, channel and/or strip.

Figure 2 shows a schematic diagram of the optical splitter 120 of Figure 1.

In the context of Figure 2, the four waveguides 104, 106, 108 and 110 are more commonly referred to as splitter waveguides. The four splitter waveguides 104, 106, 108 and 110 have an S-bend arrangement in their respective regions 104a, 106a, 108a and 110a approaching the central waveguide 102. The radii of the S-bends, for instance R and R_1 of the splitter waveguides 104 and 106 respectively, are designed for minimum optical power loss, which is dependent on the splitter waveguides width w and the refractive index contrast ΔN of the splitter waveguides material.

The S-bend arrangement provides several advantages over a waveguide that has a straight alignment. For instance, the S-bend arrangement achieves an optical splitter with a more narrow width, thus producing an overall more compact device. Also, light travelling through the waveguide with an angled arrangement of straight waveguide portions has greater transmission loss compared to the S-bend arrangement in the example embodiment.

Substantially straight waveguides (for instance portions L_2 and L_1 of the splitter waveguides 108 and 110 respectively) are incorporated at the beginning of each of the S-bend arrangements 104a, 106a, 108a and 110a to couple optical power from the central waveguide 102 into the splitter waveguides 104, 106, 108 and 110. Optical coupling strength gradually decreases from the coupling regions 102a and 102b towards the output ends of the splitter waveguides 104, 106, 108 and 110 of the optical splitter 120.

The input ends of the four splitter waveguides 104, 106, 108 and 110 are separated a distance *Lgap*, from the central waveguide 102. On the other hand, a distance *Lsep* separates the output ends of each adjacent waveguide in the optical splitter 120. The end separation distance *Lsep* is selected to fulfill the criteria of zero power transfer between adjacent waveguides.

In operation, optical powers 112 with broad wavelengths are injected into the central waveguide 102. The coupling regions 102a and 102b is such that optical energy will be split substantially equally between each of the four splitter waveguides 104, 106, 108 and 110. The amplitude and phase of the optical field in each of the four splitter waveguides 104, 106, 108 and 110 is influenced by several waveguide parameters at the coupling regions 102a and 102b. These waveguide parameters include the waveguide width w, gap *Lgap*, height (not shown), refractive index difference (not shown) and the interactive length L_i of the four splitter waveguides 104, 106, 108 and 110, where i is an integer.

The process of manufacturing the optical splitter 120 in one example embodiment utilises recticle (masks) writing for the splitter pattern using an electron-beam pattern generator. The written pattern is then transferred through photolithography. A SOI wafer is first coated with photoresist, followed by the transfer of the pattern through photolithograpy. Anisotropic etching is performed to remove silicon in the exposed areas, hence creating the Si waveguides of the optical splitter 120 on the wafer. This is followed by stripping the remaining resist from the wafer.

Figure 3 shows a plot 300 of normalised power against cT, where cT is the unit of time used in the computational calculation, where c is the speed of light in vacuum

The plot 300 illustrates simulation results of the normalised power in each of the four splitter waveguides 104, 106, 108 and 110 (Figure 2) of the optical splitter 120 (Figure 2) having a silicon-on-insulator (SOI) structure with the following parameters:

w=500nm, si-overlayer = 220nm, Lgap =0.1µm, L_1 *= 3.1µm,* L_2 *=8µm, Lsep = 0.7µm*

The Finite Differential Time Domain (FDTD) Method was used to observe the power transfer effect occurring in the optical splitter 120 (Figure 2). This method is useful for analysis of small cross sectional wave-guiding structures. First, modal analysis is used to solve the fundamental mode in a photonic wire. This fundamental mode is then used as a launch file to solve for the optical splitter structure in question. This way, the loss of the structure in question is computed due to device configuration and not the loss inherent by the waveguide structure caused by modal mismatch.

Numerals 302 and 304 indicate overlapping curves for the simulation results obtained from the splitter waveguides 104, 110 and 106, 108 (Figure 2) respectively. In other words, the curves for the pair 306 of waveguides 104, 110 (Figure 2) overlap, and the curves for for the pair 308 of waveguides 106, 108 (Figure 2) overlap. Figure 3 illustrates that each of the four splitter waveguides 104, 106, 108 and 110 (Figure 2) has an output normalised power of approximately 0.22. The result obtained agrees well with calculation based on parallel coupling using coupled mode theory.

Coupled mode theory specifies that when two waveguides are brought close together, optical modes of each waveguides either couple or interfere with each other. The coupled mode equations are given by:

$$\frac{dA}{dz} = -jk_{12}B\exp[-j(\beta_2 - \beta_1)z] \qquad (1)$$

$$\frac{dB}{dz} = -jk_{21}A\exp[-j(\beta_2 - \beta_1)z] \qquad (2)$$

where β is the propagation constant. The solutions, with the assumption of β_1 and β_2 are greater than zero, can be expressed as:

$$A(z) = \left[a_1 e^{-jqz} + a_2 e^{-jqz}\right]\exp(-j\delta z) \qquad (3)$$

$$B(z) = \left[b_1 e^{-jqz} + b_2 e^{-jqz}\right]\exp(j\delta z) \qquad (4)$$

where q is an unknown parameter to be determined. Constants a_1, a_2, b_1, and b_2 should satisfy the initial conditions:

$$a_1 + a_2 = A(0) \qquad (5)$$

$$b_1 + b_2 = B(0) \qquad (6)$$

Substituting Eqs. (3) and (4) into Eqs. (1) and (2) and applying the initial conditions from Eqs. (5) and (6) yield the following equations:

$$A(z) = \left\{ \left[\cos(qz) + j\frac{\delta}{q}\sin(qz) \right] A(0) - j\frac{\kappa}{q}\sin(qz)B(0) \right\} \exp(-j\delta z) \qquad (7)$$

$$B(z) = \left\{ -j\frac{\kappa}{q}\sin(qz)A(0) + \left[\cos(qz) - j\frac{\delta}{q}\sin(qz) \right] B(0) \right\} \exp(j\delta z) \qquad (8)$$

where q is given by $q = \sqrt{\kappa^2 + \delta^2}$ and k is the coupling coefficient.

If light is coupled into the adjacent waveguide only at z=0, this yields the conditions of $A(0)=A_o$ and $B(0)=0$. The optical power flow along the z-direction is given by:

$$P_a(z) = \frac{|A(z)|^2}{|A_o|^2} = 1 - F\sin^2(qz) \qquad (9)$$

$$P_B(z) = \frac{|B(z)|^2}{|A_o|^2} = F\sin^2(qz) \qquad (10)$$

where F is the maxium power-coupling efficiency, defined by

$$F = \left(\frac{\kappa}{q}\right)^2 = \frac{1}{1 + (\delta/\kappa)^2} \qquad (11)$$

Figure 4 shows a cross sectional view of one of the four passive photonic bandgap structures 140 of Figure 1.

The passive photonic bandgap structure 140 has a SOI structure. The passive photonic bandgap structure 140 comprises a silicon layer 402 formed above an insulating SiO_2 layer 406.

The silicon layer 402 has arrays of 1-D periodic air holes 404 formed in the silicon layer 402, with a microcavity 410 breaking the periodicity of the airholes. The airholes that are immediately adjacent to the microcavity 410 are given the reference numeral 408.

The microcavity 410 acts as a defect within the silicon layer 402 that causes a state that is analogous to the formation of a level within a semiconductor bandgap. In this manner, the silicon layer 402 acts as a photonic crystal waveguide with a defect in the mid section. The light confinement capability of the microcavity 410 induces a strong electric field in the microcavity 410 which is stronger than the electric field inside the remainder of the silicon layer 402. By removing the cladding (not shown) above the microcavity 410, the induced electric field of the microcavity 410 enhances the effective cross section of analytes that are present above the surface of the photonic bandgap device 100 (Figure 1) when the photonic bandgap device 100 (Figure 1) is used as a biosensor. Thus, when an analyte is present in the vicinity of the microcavity 410, optical light being transmitted through the microcavity 140 becomes attenuated. A drop in the output power of the photonic bandgap device 100 (Figure 1) thus indicates that analytes are detected. As one microcavity 410 exists along each of the four splitter waveguides 104, 106, 108 and 110 (Figure 1), the passive sensor device 100 (Figure 1) can be applied, e.g. as a multiple sensing arm biosensor using only one light source and detector pair. By choosing each microcavity 410 to exhibit a different transmission wavelength, one broadband light source can be placed at the input side and a detector in the form of a spectrum analyser can be placed at the output side to monitor the response of the respective wavelengths along each respective sensing arm.

A Bragg mirror-like response is present on both sides 406a and 406b of the microcavity 410. The air holes 408 that are immediately adjacent to the microcavity 410 have a different diameter than the diameter of the remaining air holes 404. The air holes 408 are commonly referred to as the innermost air holes. Unlike conventional photonic crystal waveguides, where the air holes are etched only into the silicon layer, the air holes 404 and 408 are etched a depth within the SiO_2 layer 402. This "etch-down" design improves the transmission property of the photonic crystal waveguide 402. This "etch-down" design also prevents the wave travelling inside the silicon layer 402 from leaking into the SiO_2 layer 406. In preventing wave leakage, the "etch-down" design was found as effective as the known "air-bridge" design, where in the "air-bridge" design an air gap is formed beneath the microcavity structure. However, the "etch-down" design is simpler to fabricate.

The formation of the airholes 404 and 408 are to limit the wave vector factor inside the photonic crystal waveguide 402. The airholes 404 and 408 also produce an evanescent field that facilitates coupling of the waveguide modes in the photonic crystal waveguide to the microcavity 410.

The symbols used to demarcate the various dimensions of the photonic crystal waveguide 402 are summarised as follows: a_0 is the length of the microcavity 410; *a* is the period of the air holes; d_0 is the diameter of the two air holes 408 immediately adjacent to the microcavity 410; *d* is the diameter of the remaining air holes 404; *w* is the width of the photonic crystal waveguide 402; t_1 is the thickness of the photonic crystal waveguide 402; t_2 is the etching depth of the SiO_2 layer 406; and *h* is the etching depth of the air holes 404 and 408.

From running simulations using a 3-D FDTD package from CST Microwave Studio, it was found that an optimum etching depth *h* for the air holes 404 and 408 was 400nm, which produced a Q factor of around 320, for a_0=295nm, a=180nm, d_0=80nm, d=68nm, w=475nm, t_1=400nm and t_2=400nm. The Q factor is a measure of the strength of the relative linewidth. The Q factor is the ratio of the resonance frequency, v and the (full width at half maximum) bandwidth dv of the resonance, i.e.

Q factor = v/dv (12)

Varying the etching depth *h* from 400 nm to 550 nm did not provide any obvious improvement, where the power transmission at resonance remained almost unchanged.

The transmission property for the photonic bandgap structure 140 was simulated using the 3-D FDTD package from CST Microwave Studio. An etching depth *h* of 400nm was used. The simulation was conducted using diameter d_0 values 60, 70, 80 and 90nm for the air holes 408,. and respective length a_0 values 275, 285, 295, 305 and 315nm for the microcavity 410. The results of the simulation are shown in Figure 5, for *a=180nm*, *d_0=80nm*, *d=68nm*, *w=475nm*, t_1=400nm and t_2=400nm.

Figure 5 shows a plot 502 of the transmission 506 and Q factor 508 against the diameter d_0 of the innermost air holes 408 of the photonic bandgap structure 140 of Figure 4. Figure 5 also shows how varying the length a_0 of the photonic bandgap structure 140 (Figure 4) affects both the transmission 506 and the Q factor 508 characteristics of the photonic bandgap structure 140 (Figure 4). Graphs 520, 521, 522, 523 and 524 show the range of transmission 506 and Q factor 508 values for varying the diameter d_0 for cavity lengths a_0 of 315, 305, 295, 285 and 275 nm respectively.

From Figure 5, it can be observed that the Q factor 508 decreases when the length a_0 increases. This is because the optical mode is not as well confined in the microcavity 410 (Figure 4) when the length a_0 increases. Transmission 506 characteristics improve when the length a_0 is increased. The Q factor 508 reduces when the diameters d_0 are reduced. When the diameter d_0 is reduced, the optical throughput also increases. Thus, the transmission 506 and Q factor 508 characteristics share an inverse relationship.

The above simulation results are summarised in Table 600 shown in Figure 6. Both the transmission 506 values and the Q factor 508 values of Figure 5A are tabulated in table 520 against their respective lengths a_0 and diameters d_0. The transmission 506 values are placed in brackets in table 600. It will be appreciated, from table 600, that a range of device parameters can be chosen to obtain a high Q factor 508 and high transmission 506 properties by tuning the microcavity length a_0 and the air holes diameters d_0. For example, when length a_0 = 295 nm and diameter d_0 = 80 nm, we obtain a Q factor 508 of around 325 and a corresponding transmission 506 of around 90%. Another example would be when length a_0 = 275 nm and diameter d_0 = 70 nm, we obtain a Q factor 508 of around 333 and a corresponding transmission 506 of around 91%. .

For a sub-micrometer height of 400nm, high scattering loss is dominated by the microcavity 410 (Figure 4) waveguide sidewall roughness. The documents "Low loss ultra-small branches in a silicon photonic wire waveguide," *IEICE Trans. Electron.*, vol. E85-C, pp. 1033-1038, 2002 by Sakai *et al.* and "Effect of size and roughness on light transmission in a Si/SiO_2 by Lee *et al.* discuss the relationship between waveguide losses and waveguide dimensions to enable the design and fabrication of a waveguide in SOI with minimal loss, where 0.1 dB/cm transmission loss was demonstrated for a device with a Si layer height of 200 nm in the latter document. As such, it is feasible to use a 400nm thick Si layer (t_1) for the microcavity 410.The results discussed above pertain to TE polarization optical signals in the example embodiments. However, polarisation independent SOI waveguides can also be formed, e.g. based on the technique described in S. P. Chan, C. E. Png, S. T. Lim, G. T. Reed, V. M. N. Passaro, "Single Mode and Polarisation Independent Silicon-on-Insulator Waveguides with Small Cross Section", IEEE J. of Lightwave Tech.. **23**, 2103-2111 (2005). Polarization independent waveguides may be incorporated in different embodiments for fabrication of polarization independent devices.

Figure 7 shows a schematic diagram of the optical combiner 180 of Figure 1. It will be appreciated that the optical combiner 180 has an inverse configuration to the optical splitter 120 of Figure 2. Thus, the optical combiner 180 has corresponding parameters to that of the optical splitter 120 (Figure 2).

In the context of Figure 7, the four waveguides 104, 106, 108 and 110 are more commonly referred to as combiner waveguides. The four combiner waveguides 104, 106, 108 and 110 have an S-bend arrangement in their respective regions 104b, 106b, 108b and 110b approaching the output portion of the central waveguide 102. The radii of the S-bends, for instance R and R_1 of the combiner waveguides 110 and 108 respectively, are designed for minimum optical power loss, which is dependent on the combiner waveguides width *w* and the refractive index contrast ΔN of the combiner waveguide material.

Substantially straight waveguides (for instance portions LO_2 and LO_1 of the splitter waveguides 106 and 104 respectively) are incorporated at the end of each of the S-bend arrangements 104b, 106b, 108b and 110b to couple optical power from each of the splitter waveguides 104, 106, 108 and 110 into the central waveguide 102.

The output ends of the four combiner waveguides 104, 106, 108 and 110 are separated a distance *LOgap*, from the central waveguide 102. On the other hand, a distance *LOsep* separates the beginning portions of each adjacent waveguide in the optical combiner 180. The separation distance *LOsep* is selected to fulfill the criteria of zero power transfer between adjacent waveguides.

Figure 8 shows a plot 800 of normalised power against cT. The plot 800 illustrates results, using the FDTD simulation method, of the total normalised output power from the central waveguide 102 of the optical combiner 180 of Figure 8. The simulated optical combiner 180 (Figure 7) had a silicon-on-insulator (SOI) structure with the following parameters:

w=500nm, si-overlayer = 220nm, Lgap =0.1µm, L_1 *= 3.1µm,* L_2 *=8µm, Lsep = 0.7µm*

The FDTD simulation was conducted to investigate the effectiveness of the optical coupling between the four combiner waveguides 104, 106, 108 and 110 and the central waveguide 102. Curve 802 shows that the output from the optical combiner 180 has a normalised power of 0.95.

It will be appreciated that the optical splitter and the optical combiner discussed above can be used in a number of device applications, including, e.g. in optical multiplexers and optical demultiplexers.

Figure 9 shows a schematic diagram of an optical demultiplexer 900 built in accordance with one embodiment of the invention.

The optical demultiplexer 900 shown in Figure 9 is of the 4 channel configuration. However, it will be appreciated that it is possible to realise an N=4, 6, 8, 10, ...etc channel configuration with the appropriate design consideration, in different embodiments. The optical demultiplexer 900 has an optical splitter 920 having a central waveguide 902 and four waveguides 904, 906, 908 and 910. A photonic bandgap structure 940 is formed in each of the four waveguides 904, 906, 908 and 910.

Optical energy injected into the central waveguide 902 will be equally split into each of the four waveguides 904, 906, 908 and 910. The photonic bandgap structure 940 acts as an optical filter for the respective channel wavelengths.

Figure 10 shows a schematic diagram of an optical multiplexer 1000 built in accordance with one embodiment of the invention.

The optical multiplexer1000 shown in Figure 10 is of the 4 channel configuration. . However, it will be appreciated that it is possible to realise an N=4, 6, 8, 10, ..etc channel configuration with the appropriate design consideration, in different embodiments. The optical multiplexer 1000 has an optical combiner 1080 having a central waveguide 1002 and four waveguides 1004, 1006, 1008 and 1010. A photonic bandgap structure 1040 is formed in each of the four waveguides 1004, 1006, 1008 and 1010.

The photonic bandgap structure 1040 acts as an optical filterfor the respective channel wavelengths. Resulting optical energy that is transmitted from each photonic bandgap structure 1040 on each of the four waveguides 1004, 1006, 1008 and 1010 will be combined into the central waveguide 1002.

In another application, the optical splitter and combiner can be used in an active attenuation device 1100 as shown in Figure 11 for one embodiment of the invention.

The active attenuation device 1100 has an optical splitter 1120 at the input end and an optical combiner 1180 at the output end.

The active attenuation device 1100 shown in Figure 11 is of the 1X4 splitter configuration, where the active attenuation device 1100 comprises a central waveguide 1102 and four waveguides 1104, 1106, 1108 and 1110. A pair of the waveguides 1104, 1106, 1108 and 1110 is disposed on each side of the central waveguide 1102. An active photonic bandgap structure 1140 is formed in each of the four waveguides 1104, 1106, 1108 and 1110 between the optical splitter 1120 and the optical combiner 1180.

The active attenuation device 1100 has a 1x4 splitter configuration. However, it is possible to realise a 1xN, N=4, 6, 8, 10, ...etc splitter configuration with the appropriate design consideration, in different embodiments.

It will be appreciated that the optical splitter 1120 and the optical combiner 1180 have similar structures, dimensions and fabrication methodology to both the optical splitter 120 and the optical combiner 180 of Figure 1 respectively. The active photonic bandgap structure 1140 includes a photonic bandgap structure similar to the photonic bandgap structure 140 of Figure 1, but the microcavity 1140a of the active photonic bandgap structure 1140 has adjacent cathode and anode regions 1140b and 1140c.

Figure 12 shows a cross sectional view of a microcavity 1140a of the active attenuation device 1100 of Figure 11.

The cathode and anode regions 1140b and 1140c, and the microcavity 1140a are formed above a SiO_2 layer 1206, where both the cathode region 1140b and the anode region 1140c are adjacent to and in contact with the microcavity 1140a. The SiO_2 layer 1206 is formed above a Si substrate 1246.

In one example embodiment, fabrication of the p+ (anode) and n+ (cathode) contacts 1140c, 1140b will now be described. Initially, the designated n+ region is covered by deposition of a 500nm oxide layer by oxidation using plasma enhanced chemical vapour deposition (PECVD), and exposingonly the designated p+ region through patterning and etching.

The p+ region is realised with the growth of 400nm of highly doped Si in the exposed region by selective epitaxy at 1×10^{20}atoms/cm^3 (Boron). In instances where the epitaxy equipment used has a limited target concentration (e.g. can only reach up to 1×10^{19}atoms/cm^3), an implantation step of Boron at an appropriate dosage to increase the net dopant concentration to 1×10^{20} atoms/cm^3 can be included. The p+ region is then protected with 500nm silicon dioxide using PECVD.

The silicon dioxide at the designated n+ region is then etched off. The n+ region is realised with the growth of 400nm of highly doped Si in the exposed region by selective epitaxy at 1×10^{20}atoms/cm^3 (Arsenic and Phosphorous). In instances where the epitaxy equipment used has a limited target concentration (e.g. can only reach up to 1×10^{19}atoms/cm^3), and an implantation step of Arsenic or Phosphorus at an appropriate dosage to increase the net dopant concentration to 1×10^{20} atoms/cm^3 can be included. The n+ region is then protected with 500nm silicon dioxide using PECVD.

Where dopant implantation is performed in the fabrication of the n+ region, the p+ region, or both, an appropriate annealing step may be required to restore the crystal lattice to its original state and to activate the implanted carriers.

Next, a layer of 300nm oxide is deposited over the wafer and then planarised using chemical mechanical polishing (CMP) in preparation of metallisation using deposition contact lithography and dry etching, followed by an alloy and anneal at 350 °C for 30 mins, to segregate the anode and cathode regions.

It is noted that the fabrication order of the n+ and p+ regions can be interchanged to increase flexibility in different embodiments.

Collectively, the anode region 1140c, the microcavity 1140a and the cathode region 1140b form an active p-i-n diode 1248. The active diode 1248 provides optical switching capability via the free carrier injection effect. This involves biasing the active diode 1248 so that carriers are injected into the microcavity 1140a which causes attenuation of the optical signal being transmitted through the microcavity 1140a.

In the embodiment shown in Figure 12, the cathode region 1140b and the anode region 1140c are highly doped regions with constant doping concentrations of 10^{20} cm^{-3}. The SiO_2 layer 1206 and the active diode 1248 each have a thickness of around 400nm. The cathode region 1140b and the anode region 1140c have a width of around 500nm each, while the microcavity 1140a has a width of around 475 nm. The microcavity 1140a has a length a_0.

The dc and transient characteristics of the active diode 1248 was investigated using a 2-D ATLAS device simulation package from SILVACO. The results are discussed with reference to Figures 13, 14 and 15.

Figure 13 shows a plot 1300 of drive voltage (V) against drive current (I) and a respective change in refractive index, Δn.

Curve 1302 shows the I-V relationship for the active diode 1248 of Figure 12. From curve 1302, it is observed that in the OFF state, i.e. when there is no carrier injection into the active diode 448, there is no change in the refractive index, Δn. In the ON state, designated here as where N_e (concentration of electrons) = N_h (concentration of free holes) ≈ 3×10^{17} cm^{-3}, there is a change in refractive index, Δn, of approximately

10^{-3}. The applied current and voltage required to achieve the ON state are 0.92 volts and 0.0879 μA respectively, corresponding to an applied power of around 80.9 nW.

Curve 1304 shows the static performance of the active diode 1248 of Figure 12, which indicates the change in refractive index, Δn, and hence phase change, varies nonlinearly with the applied current. One factor, which contributes to the nonlinearity of the change in phase versus current density relationship, is the sublinear dependence of the change in concentration of the free holes, ΔN_h, with the change in refractive index, Δn. As the active diode 1248 is driven harder, more free carriers are injected into the intrinsic region (the microcavity 1140a) of the active diode 1248. This increase in the concentration of the previously intrinsic region results in an increase in the Auger recombination rate (at injected carrier concentrations much greater than 10^{17} cm^{-3} the Auger recombination becomes the dominant recombination process). This results in a reduced carrier lifetime in the intrinsic region. The active diode 1248 has thus to be driven harder to achieve an equivalent refractive index change, Δn, than at lower drive powers. An increase in the recombination rate will result in the active diode 1248 becoming a faster switching device, i.e. a reduction in the rise and fall times of the active diode 1248.

Figure 14 shows a plot of attenuation (dB) against drive current (μA). Curve 1402 shows the attenuation experienced by an optical signal propagating through the microcavity 1140a of Figure 12 of length a_0 275nm. From Figure 14, it is observed that attenuation increases as the active diode 1248 is driven harder.

For example, by driving the device to produce an injection level off 3.9 X 10^8, which corresponds to an applied voltage of around 1.05V, the attenuation is given by:

$$\Delta\alpha = \Delta\alpha_e + \Delta\alpha_h \qquad (13)$$

$$= 8.5 \times 10^{-18}.\Delta N_e + 6.0 \times 10^{-18}.\Delta N_h$$

$$= 8.5 \times 10^{-18}.(3.9 \times 10^{8}) + 6.0 \times 10^{-18}.(3.9 \times 10^{8})$$

$$= 56.3 cm^{-1}$$

This is equivalent to 244 dB/cm, which is in turn equivalent to 6.72e-3 dB for the microcavity 1140a (Figure 12) length a_0 of 275nm, or 1.34e-2 dB for a microcavity 1140a (Figure 12) length a_0 of 550 nm. Such attenuation is about 5 orders of magnitude greater than existing attenuators, such as existing fiber based photonic bandgap attenuators or Si rib or strip waveguide based attenuators. It will also be appreciated that attenuation can be increased by lengthening the microcavity 1140a (Figure 12).

Figure 15 shows a plot 1500 of the change in refractive index, Δn, against transient time for the active diode 1248 of Figure 12. The plot 1500 is used to evaluate the dynamic performance of the active diode 1248 (Figure 12) by investigating the switching speed exhibited by a transient modelling solution. Both the anode region 1140c (Figure 12) and the cathode region 1140b (Figure 12) were first zero biased 1502 for 10 ns, followed by a step increase 1504 to a voltage V_π for 200ns, and a subsequent step decrease 1506 to a voltage 0V. V_π is the voltage corresponding to a 180° phase shift and is about 0.92V from Figure 13. The rise time, t_r, is defined as the time required for the induced phase shift to change from 10% to 90% of the maximum value. Likewise, the fall time, t_f, is defined as the time required for the induced phase shift to change from 90% to 10% of the maximum value. For the active diode 1248 (Figure 12), the rise and fall times were determined to be t_r = 0.215ns and t_f = 0.043ns respectively.

The dynamic optical absorption introduced by switching the device ON (step increase 1204) corresponds to $N_e = N_h \approx 3\times10^{17}\,cm^{-3}$. Using equation (14), $\Delta\alpha = \Delta\alpha_e + \Delta\alpha_h = 8.5\times10^{-18}(\Delta N_e) + 6.0\times10^{-18}(\Delta N_h)$ (14)

where ΔN_e (cm^{-3}) is the electron concentration change; ΔN_h (cm^{-3})is the hole concentration change; $\Delta\alpha_e$ (cm^{-1}) is the absorption coefficient variation due to ΔN_e; and $\Delta\alpha_h$ (cm^{-1}) is the absorption coefficient variation due to ΔN_h, this injection of both electrons and holes translate to an additional absorption loss of approximately 4.35cm^{-1} (i.e. 18.9dB/cm). This results in a dynamic optical absorption of approximately 0.0005dB if the microcavity 1140a (Figure 12) length a_0 is around 275nm.

The optical attenuation can be improved by optimising the position of the dopant contact windows for both the anode region 1140c (Figure 12) and the cathode region 1140b (Figure 12). The active diode 1248 (Figure 12) switching performance can also be improved, without changing its physical dimensions, by overdriving during the rise and fall times (steps 1204 and 1206 respectively). However, overdriving has the disadvantage of increasing the complexity of the active attenuation device 1100 (Figure 11).

In another application, phase modulation can be introduced into a waveguide arm. Figure 16 shows a schematic diagram of an active phase modulator MZI 1600 built in accordance with one embodiment of the invention.

The active phase modulator MZI 1600 has an optical splitter 1620 having a central waveguide 1602 and four waveguides 1604, 1606, 1608 and 1610. An active photonic bandgap structure 1640 is formed in each of the four waveguides 1604, 1606, 1608 and 1610.

The output portion of the waveguides 1604 and 1606 are joined so that interference between the optical field transmitted in each waveguide 1604 and 1606 occurs at region 1650. It will be appreciated that interference also occurs in the same manner at region 1652 for the waveguides 1608 and 1610.

Photodetectors 1654 can be placed to measure the outputs from the coupling regions 1650 and 1652.While Figure 16 shows an active phase modulator MZI 1600, it will also be appreciated that a passive configuration can also be designed into another embodiment, where the active structure 1640 is replaced with a passive photonic bandgap structure 140 , such as Figure 1, for sensing applications.

Embodiments of the photonic bandgap devices described herein can be applied in different operations.

The photonic bandgap devices can be deployed in optical communications, which require devices that are low cost, have a high density and provide high data transmission rates. The devices can also be used for biosensing and optical interconnects.

Example embodiments can provide an integrated electronic chip with more waveguide arms in addition to the central waveguide. By closely packing more waveguide arms, multiple tests could be performed simultaneously. The size and sensitivity of the photonic bandgap devices facilitates nanoparticle detection and detection of sensitive analytes.

Other possible applications include diagnostic toolkits to test for GO/NOGO, as well as optical multiplexers and demultiplexers. GO/NOGO applications can be used to determine whether a functional response is met, e.g. serving as an indicator that represent a positive or negative result.

CLAIMS

1. An optical splitter comprising:

a first longitudinal waveguide for receiving an incoming light wave;

at least first and second pairs of output waveguides, the output waveguides of each pair being disposed on opposite sides of the first waveguide;

wherein each of the output waveguides of each pair comprises a longitudinal portion disposed parallel to the first waveguide and such that optical power is coupled from the first waveguide into the respective longitudinal portions and the longitudinal portions of output waveguides of the first and second pairs are displaced along a length of the first waveguide;

wherein each of the output waveguides of each pair further comprises a substantially S-shaped portion continuing from the respective longitudinal portions and such that optical power coupling between the respective S-shaped portions of output waveguides of the first and second pairs is substantially inhibited.

2. The optical splitter as claimed in claim 1, wherein the longitudinal portions of the output waveguides of each pair are disposed at substantially a same distance on the opposite sides of the first wav guide.

3. The optical splitter as claimed in claim 2, wherein the longitudinal portions of the output waveguides of both pairs are disposed at substantially the same distance on the opposite sides of the first waveguide.

4. The optical splitter as claimed in any one of the preceding claims, wherein a radius of the S-shaped portions of the output waveguides of each pair is chosen such that optical transmission losses are reduced compared to an angled alignment of waveguide portions.

5. The optical splitter as claimed in any one of the preceding claims, arranged for coupling substantially the same optical power from the light wave into the output waveguides.

6. The optical splitter as claimed in claim 5, wherein substantially all of an input power of the light wave is coupled into the output waveguides.

7. An optical combiner comprising:

a first longitudinal waveguide;

at least first and second pairs of input waveguides, the input waveguides of each pair being disposed on opposite sides of the first waveguide;

wherein each of the input waveguides of each pair comprises a longitudinal portion disposed parallel to the first waveguide and such that optical power is coupled from the respective longitudinal portions into the first waveguide and the longitudinal portions of input waveguides of the first and second pairs are displaced along a length of the first waveguide;

wherein each of the input waveguides of each pair further comprises a substantially S-shaped portion continuing from the respective longitudinal portions for receiving respective incoming light waves and such that optical power coupling between the respective S-shaped portions of input waveguides of the first and second pairs is substantially inhibited.

8. The optical combiner as claimed in claim 7, wherein the longitudinal portions of the input waveguides of each pair are disposed at substantially a same distance on the opposite sides of the first wav guide.

9. The optical combiner as claimed in claim 8, wherein the longitudinal portions of the input waveguides both pairs are disposed at substantially the same distance on the opposite sides of the first waveguide.

10. The optical combiner as claimed in any one of claims 7 to 9, wherein a radius of the S-shaped portions of the input waveguides of each pair is chosen such that optical transmission losses are reduced compared to an angled alignment of waveguide portions.

11. The optical combiner as claimed in any one of claims 7 to 10, wherein substantially all of respective input powers of the respective light waves is coupled into the first waveguide.

12. An optical device comprising:

a waveguide formed on a substrate, the waveguide comprising a photonic bandgap structure including an optical cavity region;

a highly doped cathode region formed along the waveguide and adjacent one side of the optical cavity region of the waveguide;

a highly doped anode region formed along the waveguide and adjacent an opposite side of the optical cavity region of the waveguide;

wherein the cathode region, the optical cavity region and the anode region form a p-i-n diode structure for controlling an attenuation characteristic of the photonic bandgap structure.

13. An optical device comprising:

an optical splitter comprising:

a first longitudinal waveguide for receiving an incoming light wave;

at least first and second pairs of output waveguides, the output waveguides of each pair being disposed on opposite sides of the first waveguide;

wherein each of the output waveguides of each pair comprises a longitudinal portion disposed parallel to the first waveguide and such that optical power is coupled from the first waveguide into the respective longitudinal portions and the longitudinal portions of output waveguides of the first and second pairs are displaced along a length of the first waveguide;

wherein each of the output waveguides of each pair further comprises a substantially S-shaped portion continuing from the respective longitudinal portions and such that optical power coupling between the respective S-shaped portions of output waveguides of the first and second pairs is substantially inhibited; and

a photonic bandgap structure optically connected to each output waveguide of the splitter, each photonic bandgap structure including a microcavity.

14. The optical device as claimed in claim 13, further comprising:

an optical combiner comprising:

a first longitudinal waveguide;

at least first and second pairs of input waveguides, the input waveguides of each pair being disposed on opposite sides of the first waveguide;

wherein each of the input waveguides of each pair comprises a longitudinal portion disposed parallel to the first waveguide and such that optical power is coupled from the respective longitudinal portions into the first waveguide and the longitudinal portions of input waveguides of the first and second pairs are displaced along a length of the first waveguide;

wherein each of the input waveguides of each pair further comprises a substantially S-shaped portion continuing from the respective longitudinal portions for receiving respective incoming light waves and such that optical power coupling between the respective S-shaped portions of input waveguides of the first and second pairs is substantially inhibited; and

wherein the photonic bandgap structures are formed in respective optical connections between the output waveguides of the splitter and the input waveguides of the combiner.

15. An optical device comprising:

an optical combiner comprising:

a first longitudinal waveguide;

at least first and second pairs of input waveguides, the input waveguides of each pair being disposed on opposite sides of the first waveguide;

wherein each of the input waveguides of each pair comprises a longitudinal portion disposed parallel to the first waveguide and such that optical power is coupled from the respective longitudinal portions into the first waveguide and the longitudinal portions of input waveguides of the first and second pairs are displaced along a length of the first waveguide;

wherein each of the input waveguides of each pair further comprises a substantially S-shaped portion continuing from the respective longitudinal portions for receiving respective incoming light waves and such that optical power coupling between the respective S-shaped portions of input waveguides of the first and second pairs is substantially inhibited; and

a photonic bandgap structure optically connected to each input waveguide of the combiner, each photonic bandgap structure including a microcavity.

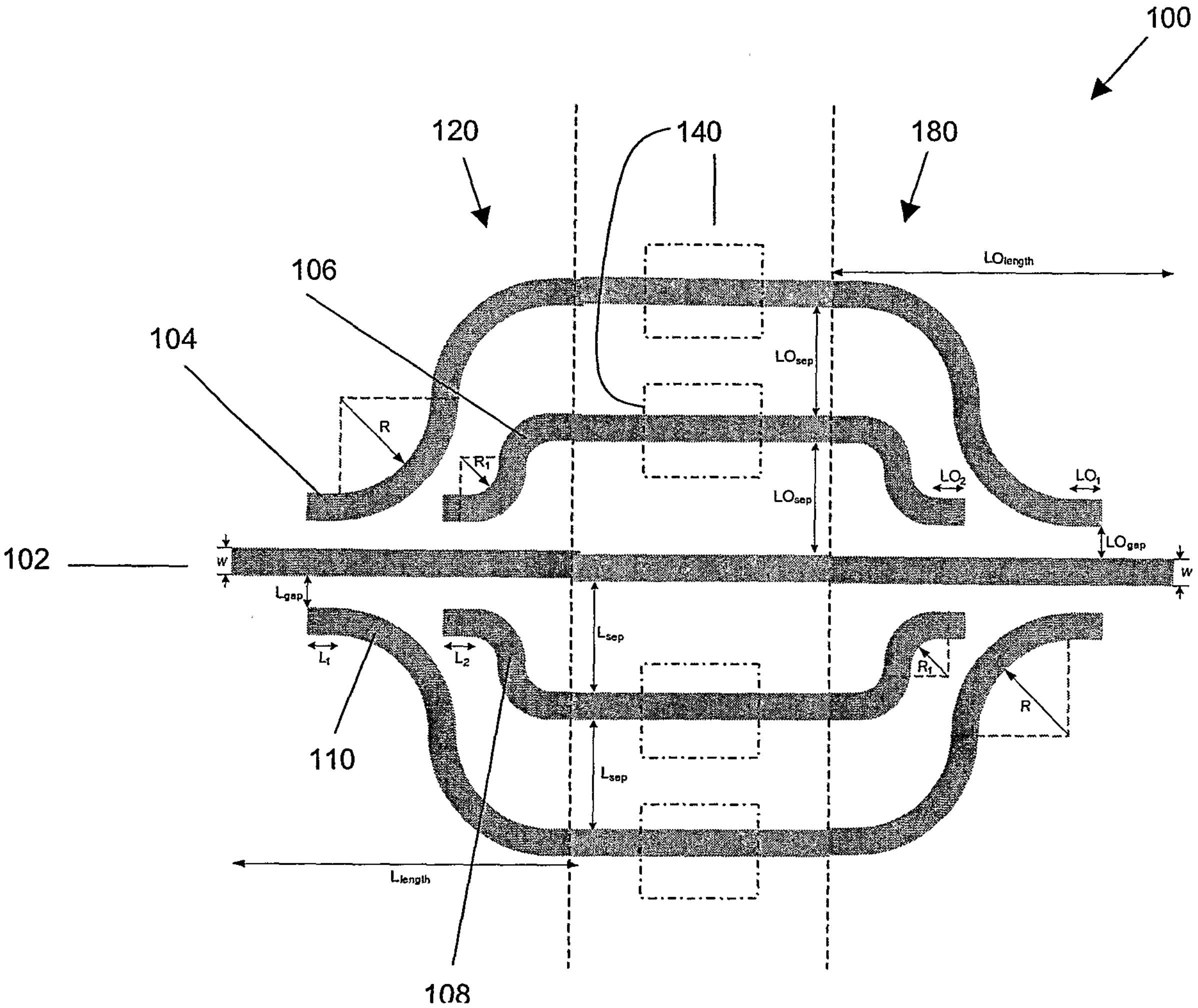

100
120
140
180
106
104
102
110
108
R
R_1
LO_{length}
LO_{sep}
LO_{sep}
LO_2
LO_1
LO_{gap}
w
w
L_{gap}
L_1
L_2
L_{sep}
L_{sep}
R_1
R
L_{length}

Figure 1

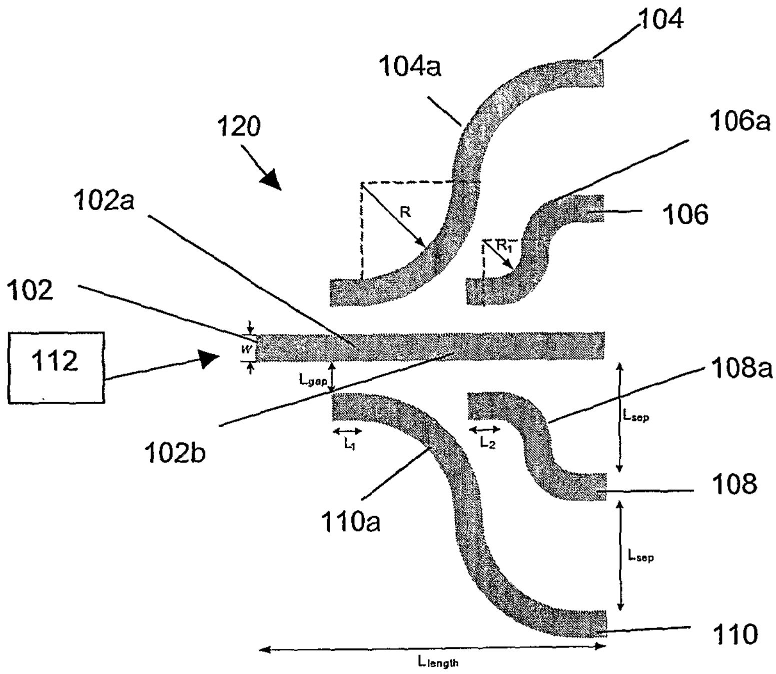

Figure 2

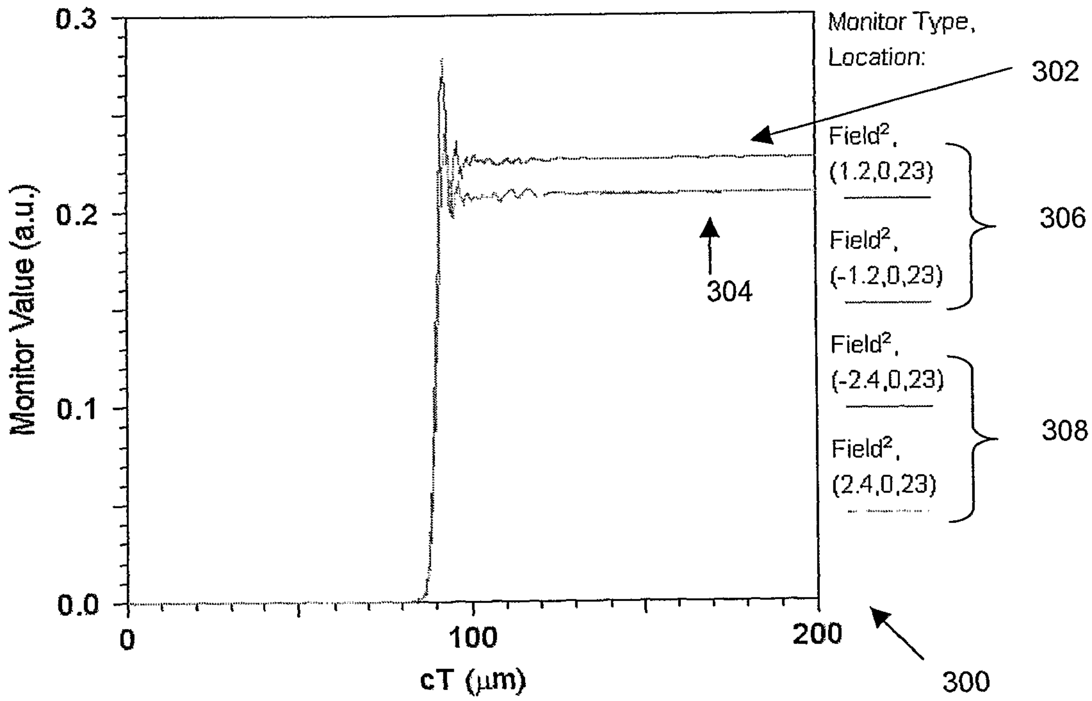

Figure 3

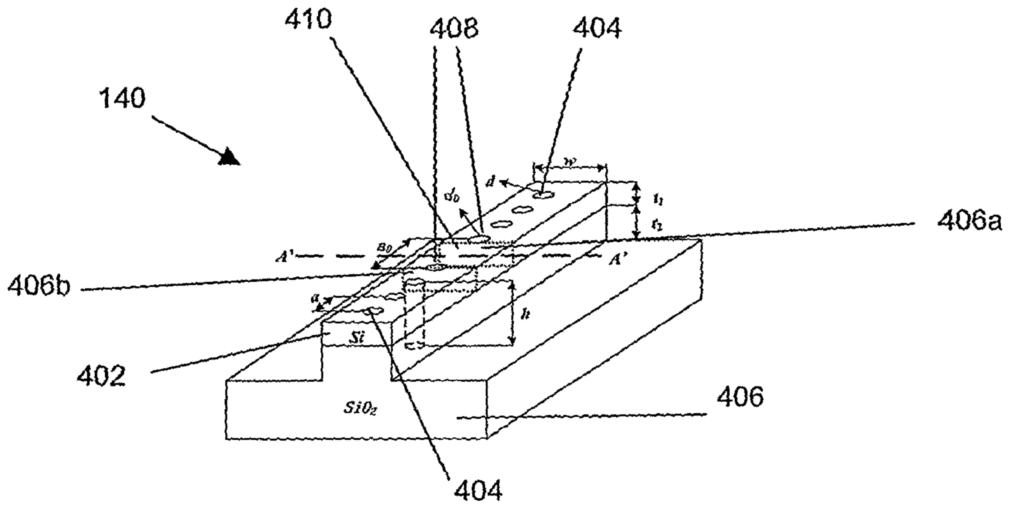

Figure 4

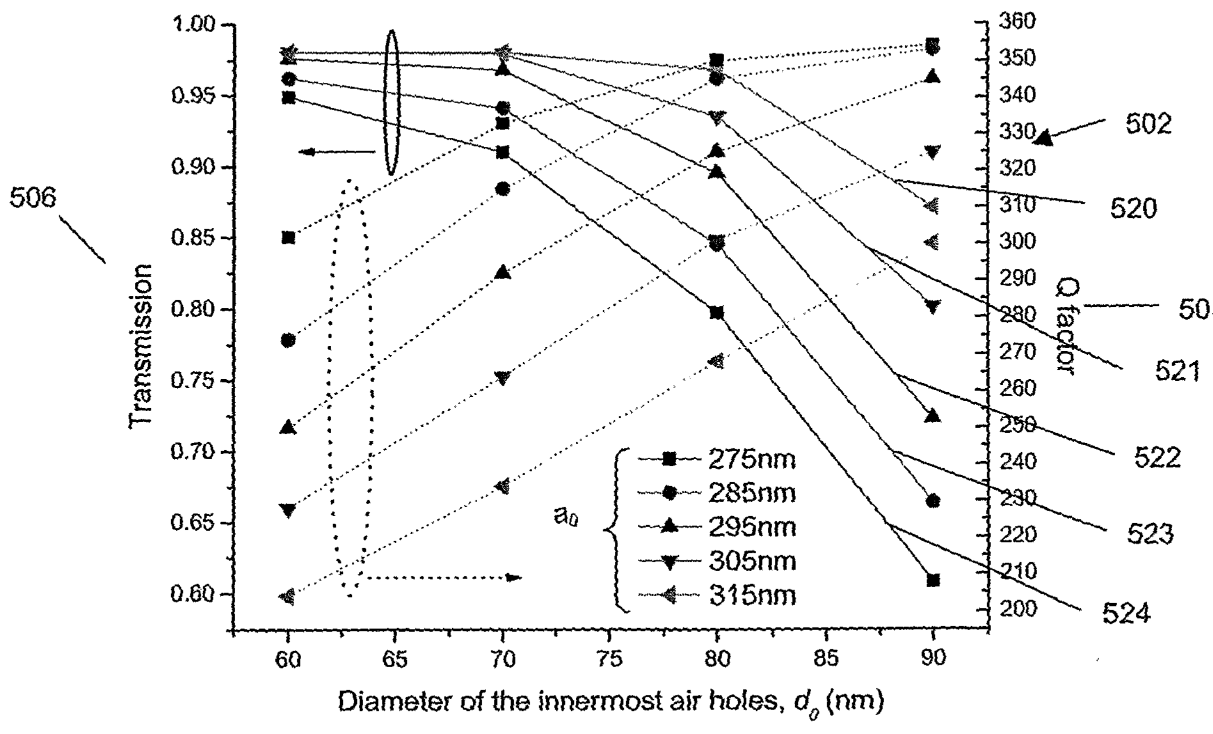

Figure 5

d_0 \ a_0	275 nm	285 nm	295nm	305 nm	315 nm
60 nm	**302 (95%)**	**274 (96%)**	**250 (98%)**	**228 (98%)**	204 (98%)
70 nm	**333 (91%)**	**315 (94%)**	**292 (90%)**	**264 (98%)**	234 (98%)
80 nm	**350 (80%)**	**345 (85%)**	**325 (90%)**	**301 (94%)**	268 (97%)
90 nm	354 (61%)	354 (66%)	345 (72%)	325 (80%)	300 (87%)

600

508

506

Figure 6

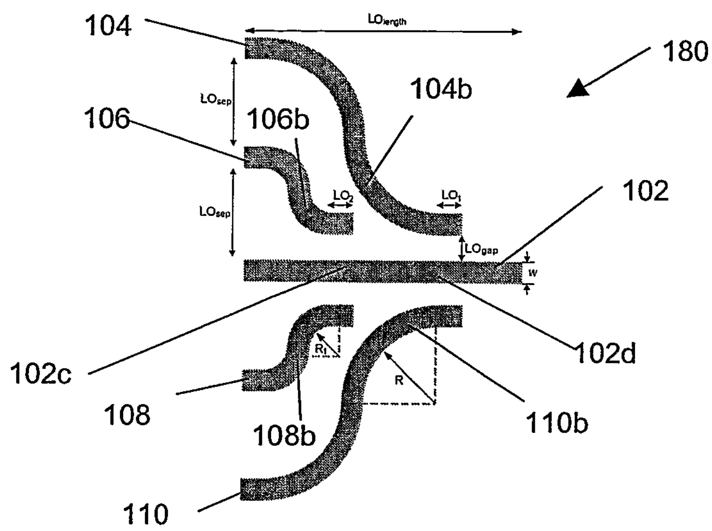

Figure 7

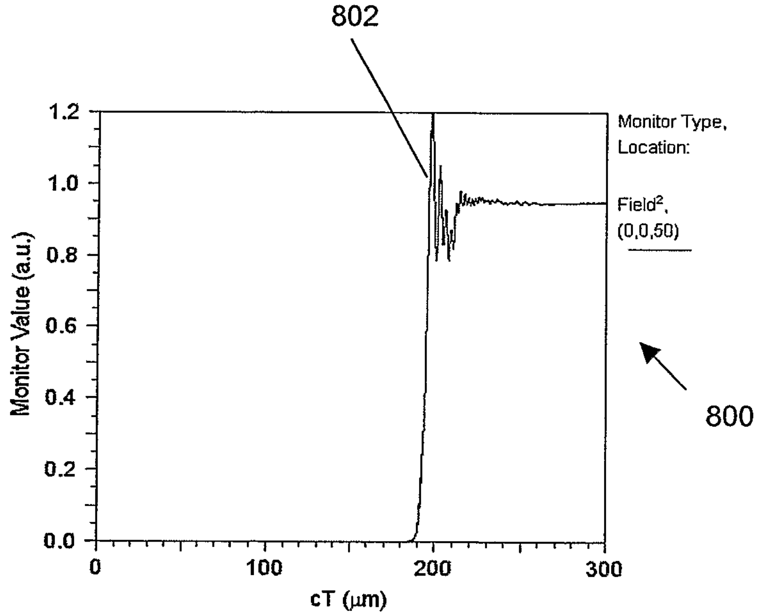

Figure 8

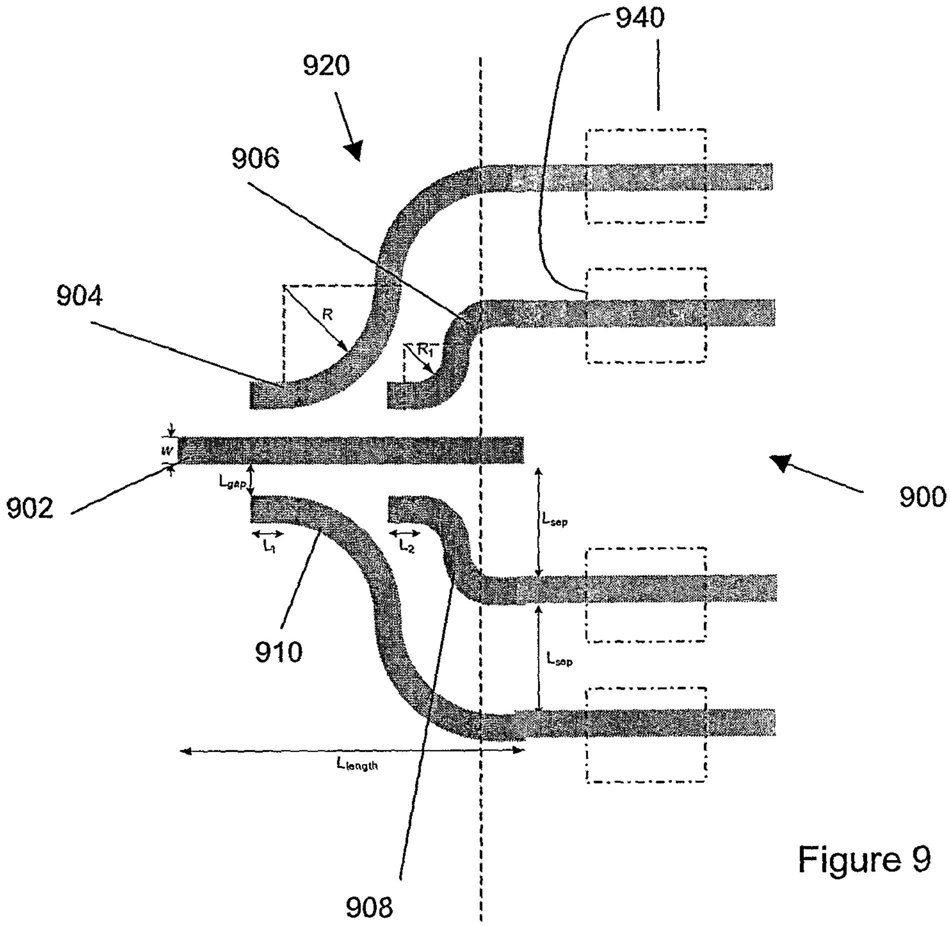

Figure 9

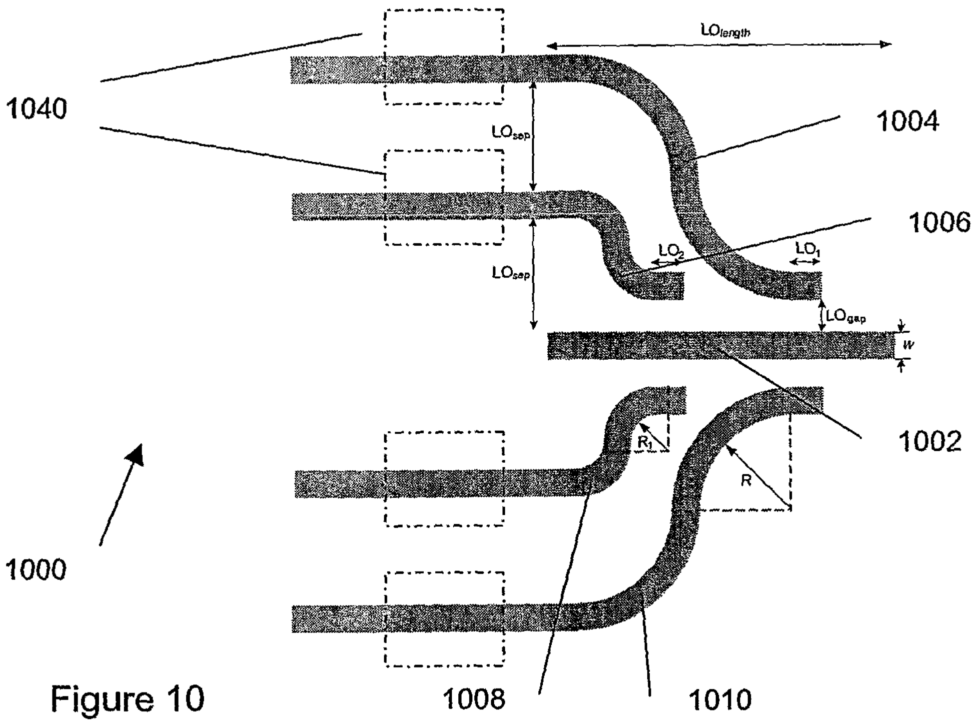

Figure 10

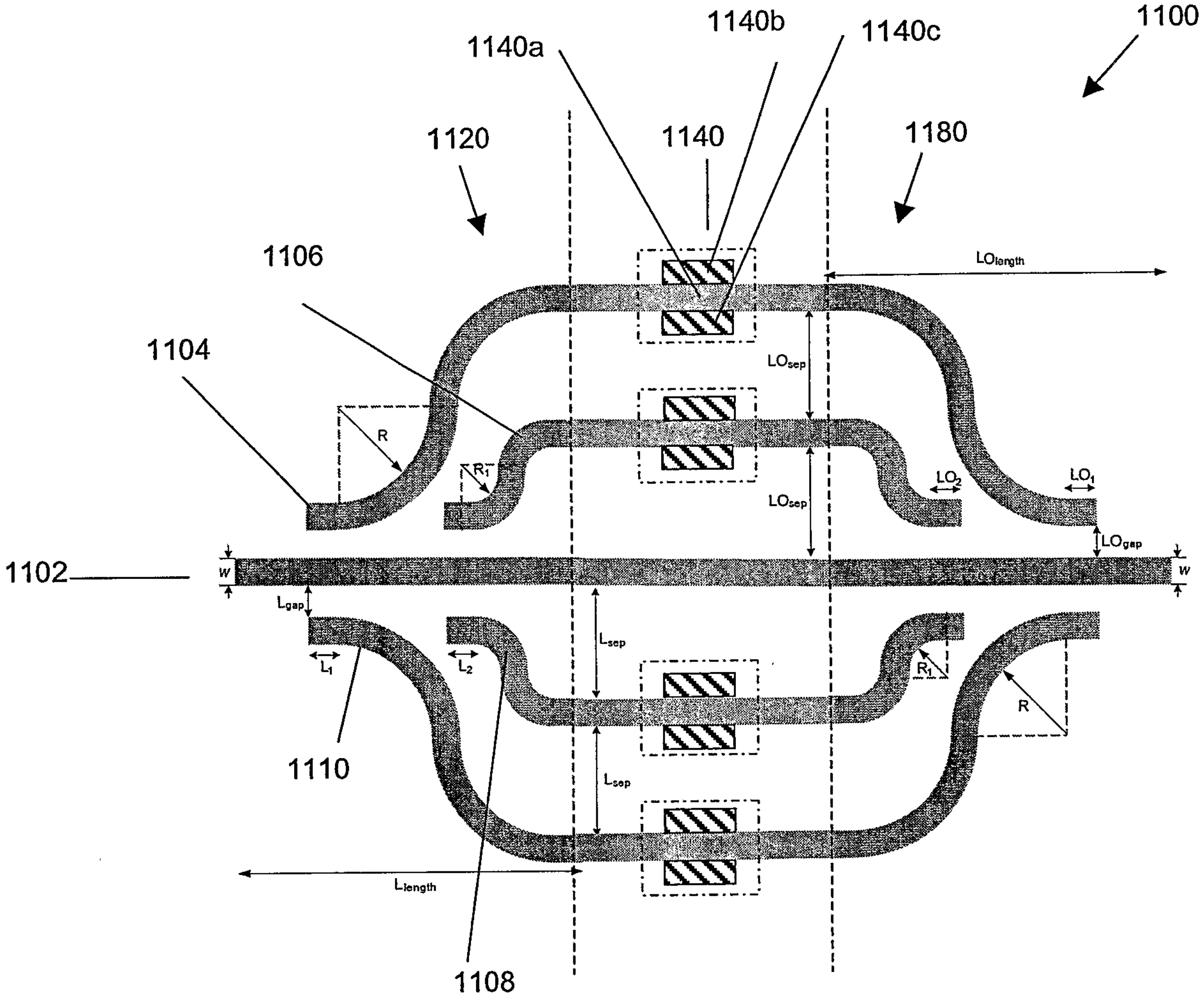
1100
1140a
1140b
1140c
1120
1140
1180
1106
1104
R
R_1
LO_{length}
LO_{sep}
LO_{sep}
LO_2
LO_1
LO_{gap}
1102
w
w
L_{gap}
L_1
L_2
L_{sep}
L_{sep}
R_1
R
1110
L_{length}
1108

Figure 11

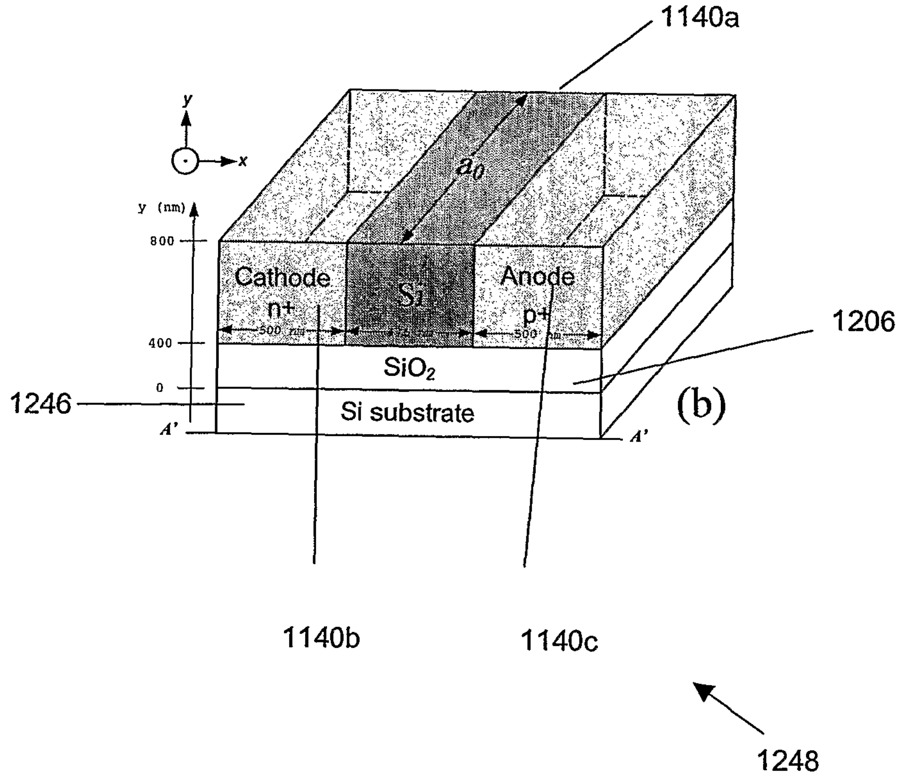
1140a
y
x
y (nm)
800
400
0
A'
a_0
Cathode
n+
Si
Anode
p+
500 nm
500 nm
1206
SiO_2
1246
Si substrate
A'
(b)
1140b
1140c
1248

Figure 12

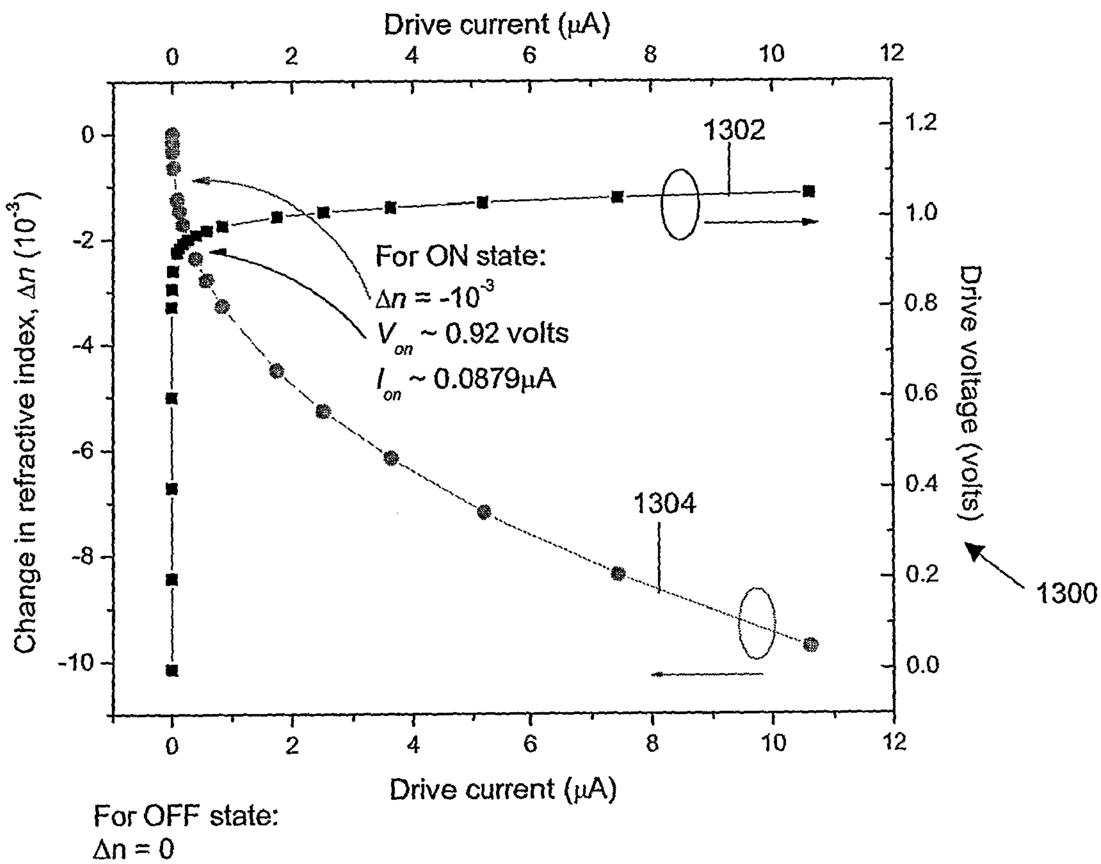
Drive current (μA)
0
2
4
6
8
10
12
0
-2
-4
-6
-8
-10
Change in refractive index, Δn (10^-3)
1.2
1.0
0.8
0.6
0.4
0.2
0.0
Drive voltage (volts)
1302
For ON state:
Δn = -10^-3
V_on ~ 0.92 volts
I_on ~ 0.0879μA
1304
1300
Drive current (μA)
For OFF state:
Δn = 0

Figure 13

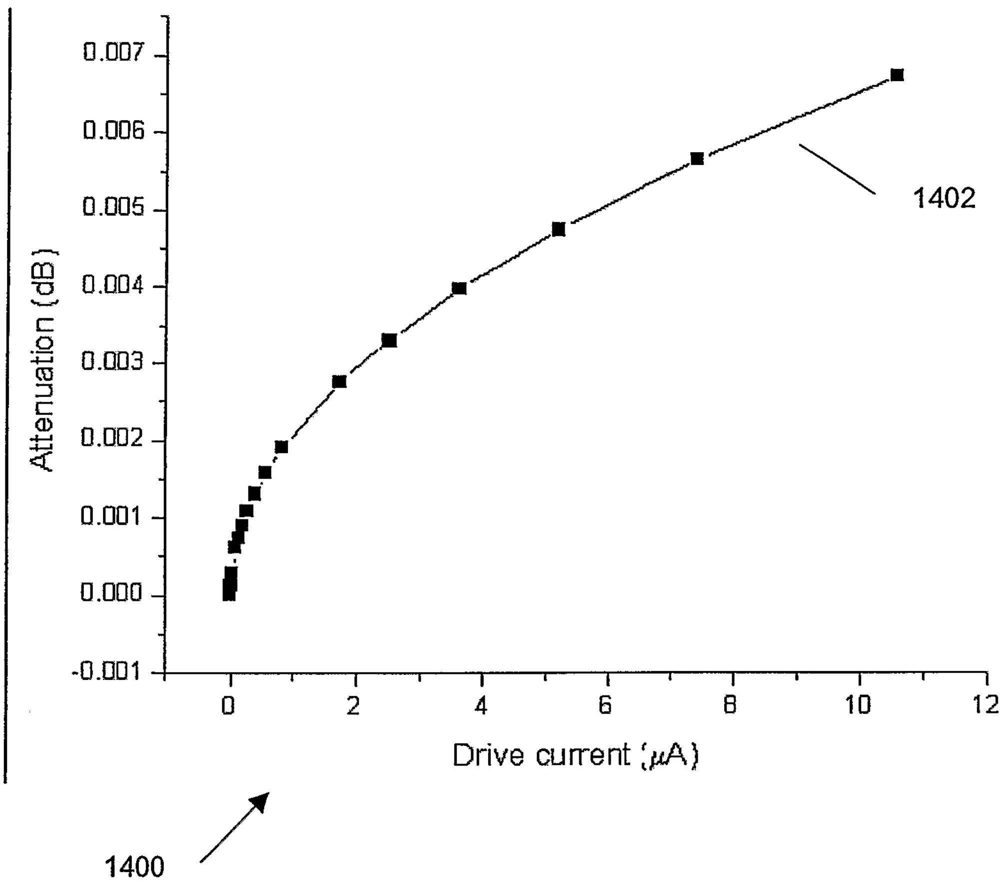
0.007
0.006
0.005
0.004
0.003
0.002
0.001
0.000
-0.001
Attenuation (dB)
0
2
4
6
8
10
12
Drive current (μA)
1402
1400

Figure 14

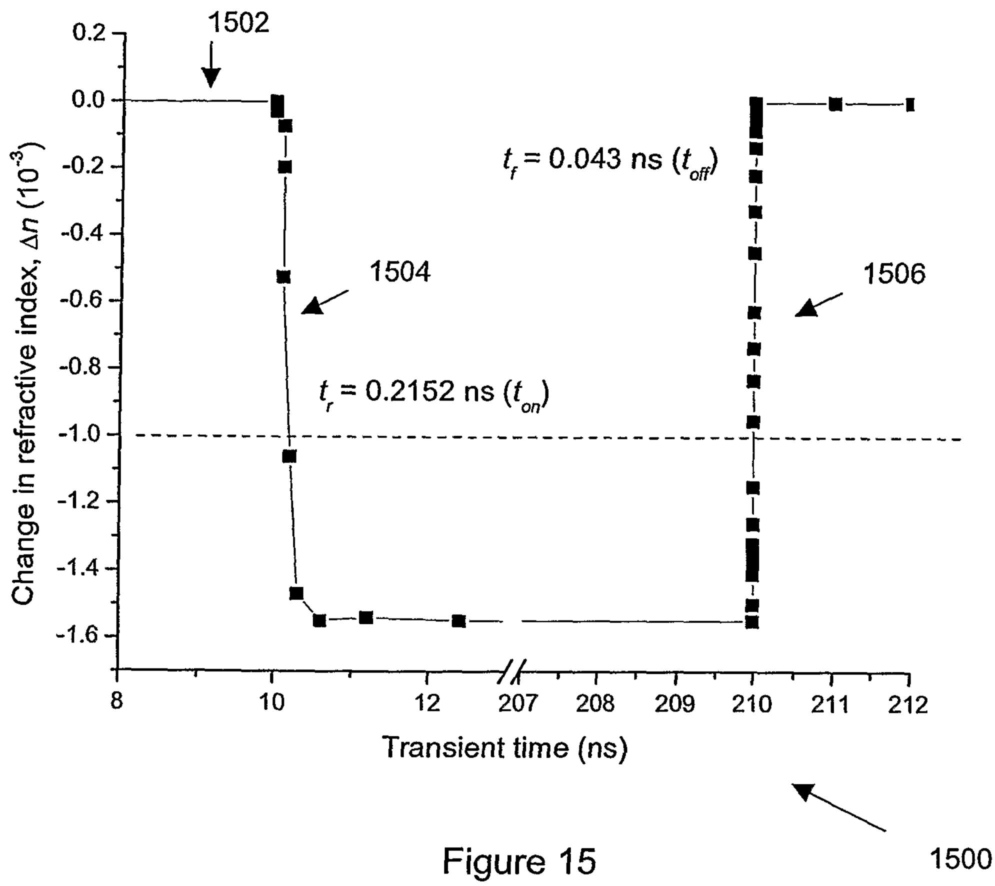
1502
1504
1506
t_f = 0.043 ns (t_{off})
t_r = 0.2152 ns (t_{on})
Change in refractive index, Δn (10^{-3})
0.2
0.0
-0.2
-0.4
-0.6
-0.8
-1.0
-1.2
-1.4
-1.6
8
10
12
207
208
209
210
211
212
Transient time (ns)
1500

Figure 15

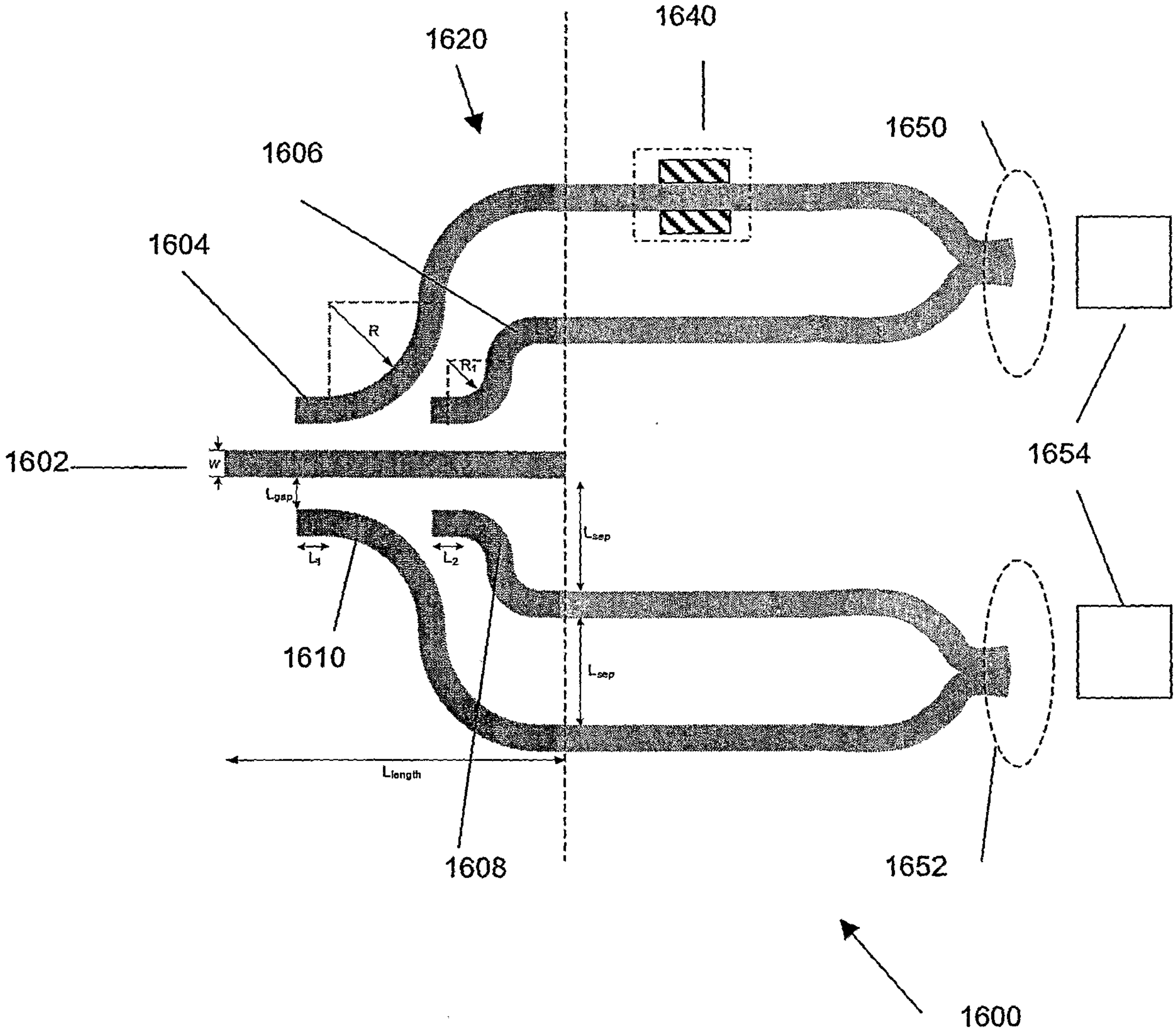
1620
1640
1650
1606
1604
R
R_1
1602
w
L_{gap}
L_1
L_2
L_{sep}
L_{sep}
1654
1610
L_{length}
1608
1652
1600

Figure 16

INTERNATIONAL SEARCH REPORT

International application No
PCT/SG2007/000174

A. CLASSIFICATION OF SUBJECT MATTER
INV. G02B6/125
ADD. G02B6/122

According to International Patent Classification (IPC) or to both national classification and IPC

B. FIELDS SEARCHED

Minimum documentation searched (classification system followed by classification symbols)
G02B

Documentation searched other than minimum documentation to the extent that such documents are included in the fields searched

Electronic data base consulted during the international search (name of data base and, where practical, search terms used)

EPO-Internal

C. DOCUMENTS CONSIDERED TO BE RELEVANT

Category*	Citation of document, with indication, where appropriate, of the relevant passages	Relevant to claim No.
X Y	US 6 201 913 B1 (YI SANG-YUN [KR] ET AL) 13 March 2001 (2001-03-13) figures 3,7 columns 6,7	1,4-7, 10,11 2,3,8,9
Y	US 4 515 428 A (FINDAKLY TALAL K [US]) 7 May 1985 (1985-05-07) figures 1-3 abstract	2,3,8,9
A	GB 2 125 184 A (PHILIPS NV) 29 February 1984 (1984-02-29) figure 1	1,7
A	EP 0 263 560 A2 (PHILIPS PATENTVERWALTUNG [DE]; PHILIPS NV [NL]) 13 April 1988 (1988-04-13) figure 1	1,7

-/--

[X] Further documents are listed in the continuation of Box C.

[X] See patent family annex.

* Special categories of cited documents :

"A" document defining the general state of the art which is not considered to be of particular relevance

"E" earlier document but published on or after the international filing date

"L" document which may throw doubts on priority claim(s) or which is cited to establish the publication date of another citation or other special reason (as specified)

"O" document referring to an oral disclosure, use, exhibition or other means

"P" document published prior to the international filing date but later than the priority date claimed

"T" later document published after the international filing date or priority date and not in conflict with the application but cited to understand the principle or theory underlying the invention

"X" document of particular relevance; the claimed invention cannot be considered novel or cannot be considered to involve an inventive step when the document is taken alone

"Y" document of particular relevance; the claimed invention cannot be considered to involve an inventive step when the document is combined with one or more other such documents, such combination being obvious to a person skilled in the art.

"&" document member of the same patent family

Date of the actual completion of the international search	Date of mailing of the international search report
21 August 2007	07/11/2007

Name and mailing address of the ISA/	Authorized officer
European Patent Office, P.B. 5818 Patentlaan 2 NL – 2280 HV Rijswijk Tel. (+31–70) 340–2040, Tx. 31 651 epo nl, Fax: (+31–70) 340–3016	Beutter, Matthias

INTERNATIONAL SEARCH REPORT

International application No
PCT/SG2007/000174

C(Continuation). DOCUMENTS CONSIDERED TO BE RELEVANT

Category*	Citation of document, with indication, where appropriate, of the relevant passages	Relevant to claim No.
A	FR 2 741 161 A1 (FRANCE TELECOM [FR]) 16 May 1997 (1997-05-16) figure 3	1,7
A	US 4 278 321 A (MACK IRIS M ET AL) 14 July 1981 (1981-07-14) figure 4	1,7
A	US 5 134 672 A (IMOTO KATSUYUKI [JP] ET AL) 28 July 1992 (1992-07-28) figures 1b,2b	1,7

INTERNATIONAL SEARCH REPORT

International application No.
PCT/SG2007/000174

Box II Observations where certain claims were found unsearchable (Continuation of item 2 of first sheet)

This International Search Report has not been established in respect of certain claims under Article 17(2)(a) for the following reasons:

1. ☐ Claims Nos.:
because they relate to subject matter not required to be searched by this Authority, namely:

2. ☐ Claims Nos.:
because they relate to parts of the International Application that do not comply with the prescribed requirements to such an extent that no meaningful International Search can be carried out, specifically:

3. ☐ Claims Nos.:
because they are dependent claims and are not drafted in accordance with the second and third sentences of Rule 6.4(a).

Box III Observations where unity of invention is lacking (Continuation of item 3 of first sheet)

This International Searching Authority found multiple inventions in this international application, as follows:

see additional sheet

1. ☐ As all required additional search fees were timely paid by the applicant, this International Search Report covers all searchable claims.

2. ☐ As all searchable claims could be searched without effort justifying an additional fee, this Authority did not invite payment of any additional fee.

3. ☐ As only some of the required additional search fees were timely paid by the applicant, this International Search Report covers only those claims for which fees were paid, specifically claims Nos.:

4. ☒ No required additional search fees were timely paid by the applicant. Consequently, this International Search Report is restricted to the invention first mentioned in the claims; it is covered by claims Nos.:

1-11

Remark on Protest

☐ The additional search fees were accompanied by the applicant's protest.

☐ No protest accompanied the payment of additional search fees.

FURTHER INFORMATION CONTINUED FROM PCT/ISA/ 210

This International Searching Authority found multiple (groups of) inventions in this international application, as follows:

1. claims: 1-11

   splitter or combiner having a specific geometry

   ---

2. claims: 12-15

   optical device comprising a waveguide comprising a photonic bandgap structure including an optical cavity region

   ---

INTERNATIONAL SEARCH REPORT

Information on patent family members

International application No
PCT/SG2007/000174

Patent document cited in search report		Publication date	Patent family member(s)			Publication date
US 6201913	B1	13-03-2001	NONE			
US 4515428	A	07-05-1985	NONE			
GB 2125184	A	29-02-1984	DE	3230657	A1	23-02-1984
			FR	2532071	A1	24-02-1984
			JP	59049506	A	22-03-1984
			US	4535440	A	13-08-1985
EP 0263560	A2	13-04-1988	DE	3634064	A1	14-04-1988
			JP	63096607	A	27-04-1988
			US	4838636	A	13-06-1989
FR 2741161	A1	16-05-1997	NONE			
US 4278321	A	14-07-1981	NONE			
US 5134672	A	28-07-1992	GB	2231412	A	14-11-1990
			JP	2277030	A	13-11-1990
			JP	2675133	B2	12-11-1997